Arabian Journal of Chemistry (2023) **16**, 104662

King Saud University

Arabian Journal of Chemistry

www.ksu.edu.sa
www.sciencedirect.com

ORIGINAL ARTICLE

Construction of macromolecular model and analysis of oxygen absorption characteristics of Hongyang No. 2 coal mine

Cong Ding [a,*], **Zongxiang Li** [a,b], **Dongjie Hu** [a], **Chuntong Miao** [c], **Bing Lu** [d], **Dameng Gao** [a]

[a] *College of Safety Science & Engineering, Liaoning Technical University, Fuxin, Liaoning 123000, China*
[b] *Key Laboratory of Mine Thermodynamic Disaster & Control of Ministry of Education, Huludao, Liaoning 125105, China*
[c] *China Coal Technology and Engineering Group Shenyang Research Institute, Fushun 113122, China*
[d] *College of Mining Engineering, Liaoning Technical University, Fuxin, Liaoning 123000, China*

Received 12 December 2022; accepted 8 February 2023
Available online 15 February 2023

KEYWORDS

Oxygen absorption characteristics;
Molecular structure model;
^{13}C NMR;
FTIR;
Molecular dynamics

Abstract Understanding the molecular structure characteristics of coal from the molecular level is of great significance for realizing rational utilization and efficient transformation of coal. The molecular structure of coal samples from 1304 working face in No.13 coal seam of Hongyang No.2 Mine (HY) was studied by industrial analysis, elemental analysis, Nuclear magnetic resonance carbon spectroscopy (^{13}C NMR) and Fourier transform infrared spectroscopy (FTIR). The results show that the aromatic compounds in coal samples of HY are mainly naphthalene ring structures. The aliphatic structure mainly consists of methyl, ethyl side chains and cycloalkanes. The ratio of aromatic bridge carbon to weekly carbon in molecular structure is 0.17. Oxygen atoms exist in the form of carbonyl, hydroxyl, and ether bonds, nitrogen atoms exist in the form of pyridine and pyrrole respectively, and sulfur atoms exist in the form of thiophene. Based on this, the planar structure model of coal macromolecule in HY is constructed, and its molecular formula is $C_{129}H_{88}O_{29}N_2S$, and its molecular weight is 2160. The structure optimization and annealing kinetics simulation of a single macromolecule model were carried out, and a stable three-dimensional coal model of HY was obtained. In addition, the oxygen absorption characteristics of coal samples in HY were studied by molecular dynamics and quantum chemistry. The results show that the adsorption capacity of the Wiser model is less than that of HY coal model. This is because, compared with the Wiser model, the content of oxygenated aliphatic hydrocarbons in the molecular structure of

---

[*] Correspondence author at: Address: College of Safety Science & Engineering, Liaoning Technical University, Fuxin, Liaoning 123000, China.
E-mail address: Dingdc123@163.com (C. Ding).

Peer review under responsibility of King Saud University.

Production and hosting by Elsevier

https://doi.org/10.1016/j.arabjc.2023.104662

HY coal is higher, and the condensation degree of polycyclic aromatic hydrocarbons is lower. Due to the stronger physical adsorption capacity of hydroxyl, ether bond, and carbonyl on O_2, HY Mine has stronger physical adsorption capacity on O_2.

1. Introduction

The pollution problem caused by spontaneous combustion of coal is becoming more and more serious, and how to use coal resources cleanly and efficiently has become a widespread concern of scholars (Xu, 2012; Qiao et al., 2022; Zhang and Zhang, 2014). It is of great significance to correctly understand the molecular structure characteristics of coal for realizing rational utilization and efficient conversion of coal (Jiang et al., 2019; Bhoi et al., 2014; Zeng et al., 2018).

In recent years, scholars have studied the molecular structure of coal by using chemical experiments and modern testing techniques and proposed more than 130 macromolecular structure models of coal (Mathews et al., 2011), such as the famous Wiser model (Wiser, 1984), Given model (Given, 1959), Shinn model (Shinn, 1996) and so on. He et al. (He et al., 2021) explored the distribution characteristics of oxygen-containing functional groups in macerals of low-rank coal; Hong et al. (Hong et al., 2021) constructed the coal char model, and simulated the combustion and gasification characteristics of coal char by reactive molecular dynamics method; Zhang et al. (Zhang et al., 2017) constructed Xishan bituminous coal macromolecular model to simulate coal molecular structure density, and its density value fitted well with the experimental data, which confirmed the rationality of the model. Meng et al. (Meng et al., 2018) constructed the structure model of Zhaozhuang coal by elemental analysis, X-ray photoelectron spectroscopy, and ^{13}C NMR, and simulated the adsorption of methane gas molecules by single molecular structure by Giant Canonical Monte Carlo (GCMC) method, providing theoretical basis for the utilization of Zhaozhuang coal resources.

At present, many scholars have used molecular simulation method to study the oxygen absorption characteristics by coal. Wu (Wu et al., 2019) used the GCMC method to analyze the ability and competitive difference of coal to adsorb CO_2, O_2, and N_2 gases according to the actual situation of fire prevention and storage of the power plant flue gas injected into goaf. Lou et al. (Lou and Jia, 2020) established a macromolecule-scale model to simulate the surface adsorption of different gases, including O_2, CO_2, and N_2 by the coal surface. Then the effect of the gas competition difference of mixed gas molecules on the surface adsorption was analyzed. Cheng et al. (Cheng et al., 2021) used density functional theory (DFT) and GCMC simulation methods to study the adsorption characteristics of CO_2, N_2, O_2, and H_2O molecules with lignite. There are few dedicated studies on the adsorption mechanism of O_2 on coal and the adsorption affinity of each functional group to O_2 molecules.

To deeply understand the molecular structure and reactivity of coal in HY Mine, the molecular structure of coal samples in No. 13 coal seam of HY Mine was studied by means of industrial analysis, elemental analysis, ^{13}C NMR and FTIR, and the molecular planar structure model was constructed. Materials studio (MS) was used to optimize the structure and annealing kinetics of the optimized model was simulated. Oxygen absorption characteristics of coal samples in HY Mine were studied by molecular dynamics and quantum chemistry. This research will provide some theoretical guidance for the anti-spontaneous combustion technology of HY Mine at the molecular level.

2. Sample preparation and experimental methods

2.1. Preparation and treatment of coal samples

The test coal was taken from 1304 working face of No.13 coal seam in the West No.3 lower mining area of Hongyang No.2 Mine of Shenyang Coking Coal Co., ltd. The coal type is lean coal. After coal samples were collected from the site, they were sealed and stored with plastic wrap immediately, and sent to the laboratory for testing and research in time.

2.2. Industrial and elemental analysis

The collected raw coal was crushed and screened to make coal samples with a particle size of 200 mesh. According to the national standard (GB/T212-2008) for industrial analysis of coal samples, according to the national standard (GB/T476-2008) for elemental analysis of coal samples, the results of industrial analysis and elemental analysis of coal samples are shown in Table 1. The calculated atomic ratios are shown in Table 2.

2.3. FTIR test

FTIR was tested by TENSOR27 FTIR spectrometer produced by Brooke Company of Germany (see Fig. 1) to study the occurrence and change of functional groups in coal samples. The resolution of FTIR spectrometer was 0.5–1 cm^{-1}, the scanning wave number ranges from 4000 to 400 cm-1, and the scanning times were 32 times. KBr laminating was used, and coal and KBr were mixed at 1:200 and then fully ground.

2.4. ^{13}C NMR test

^{13}C NMR was measured by Swiss Bruker 400 MHz nuclear magnetic resonance spectrometer (see Fig. 2) according to SY/T 5777–1995. Experimental conditions: high resolution 4.0 mm, double resonance MAS probe, rotor speed 10 kHz, pulse width 4 μs, pulse delay time 1 s, contact time 2 ms, 10,000 scans, in order to obtain the information of carbon atoms in coal samples.

Table 1 Proximate and ultimate analysis.

Industrial analysis				Element analysis				
M_{ad}/%	V_{daf}/%	A_d/%	FC_{ad}/%	C_{daf}/%	H_{daf}/%	O_{daf}/%	N_{daf}/%	S_{daf}/%
2.46	14.91	13.43	69.20	72.19	3.68	21.12	1.20	1.81

2.5. Data processing methods

According to the experimental data of industrial analysis, elemental analysis, FTIR and ^{13}C NMR, Peakfit, Origin, and other tools were used to fit the spectra, and ChemDraw was used to build and modify the coal molecular model. Based on the molecular dynamics (MD) calculation method, geometric optimization and annealing kinetics simulation were carried out. Then the lowest energy optimization model of molecular structure of coal samples in HY was obtained.

Table 2 Atomic ratio of coal sample %

Coal sample	H/C	O/C	N/C	S/C
HY	0.6117	0.2194	0.0141	0.0094

Fig. 1 FTIR Spectrometer TENSOR27.

Fig. 2 Brooke 400 M solid-state nuclear magnetic resonance instrument.

2.6. Molecular model simulation calculation

Based on the experimental data, the structural parameters of coal samples were calculated, and the coal molecular structure model of HY was constructed. The geometrical optimization and annealing dynamics of the model were simulated by MS software: the maximum iteration steps of geometrical optimization were 50000, and the energy convergence was 0.001 kcal/mol; The annealing kinetics simulation initial temperature was 300 K, the cycle steps were 10000, and five cycles were carried out. The nose temperature control method was selected to obtain the lowest energy optimization model of coal molecular structure in HY (Wu et al., 2019; Lou and Jia, 2020; Cheng et al., 2021).

3. Results and discussion

3.1. FTIR analysis

The infrared spectrum of HY coal sample is shown in Fig. 3. The absorption peaks in the infrared spectrum of coal are mainly divided into four types (Xia et al., 2019; Jiang et al., 2006; Zhang et al., 2021): The first absorption peak is located between 3600 and 3000 cm^{-1}, which is the hydroxyl absorption peak. The second is the absorption peak of fat structure between 3000 and 2800 cm^{-1}. The third absorption peak is between 1800 and 1000 cm^{-1}, which is the absorption peak of oxygen-containing functional groups. The fourth absorption peak is located between 900 and 700 cm^{-1}, which is the absorption peak of aromatic structure.

In order to analyze the types of functional groups in coal in detail, the infrared spectra are fitted by peak splitting, and the peak splitting fitting is carried out by Peakfit software, and the fitting results are shown in Fig. 4. Combined with Table 3, the main substitution modes can be determined.

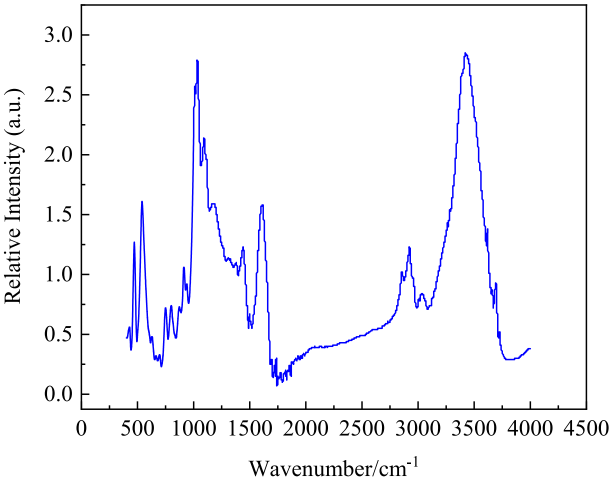

Fig. 3 FTIR test results of HY coal sample.

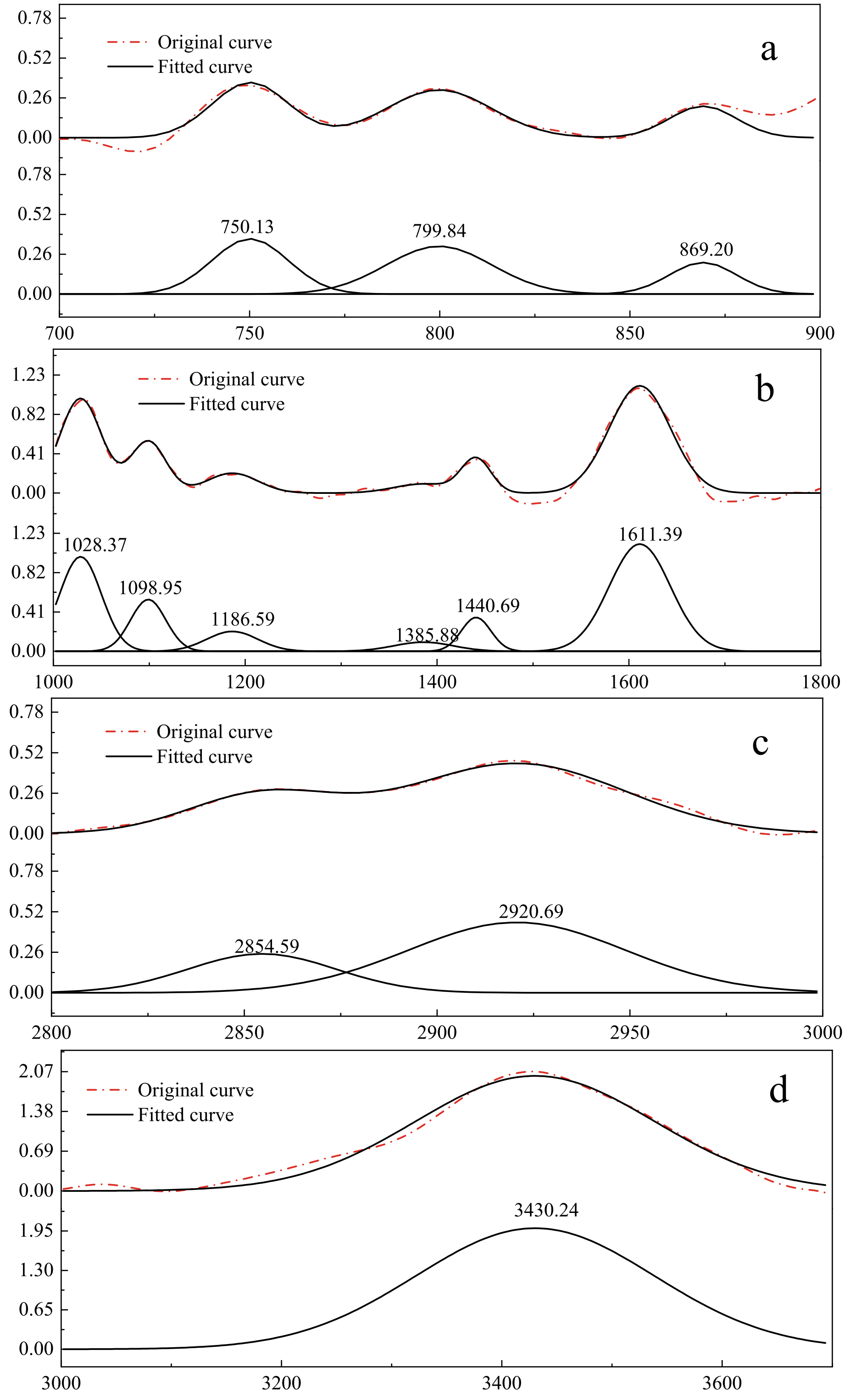

Fig. 4 Infrared spectral peak fitting of HY coal sample.

By analyzing Fig. 4 and Table 3, we can know the chemical functional groups contained in coal samples and their substitution modes. After peak fitting, there are three obvious peaks at 700 ~ 900 cm^{-1} in Fig. 4 (a), which are 1, 2 and 1, 2, 4 substituted aromatic hydrocarbons respectively. In Fig. 4 (b), six absorption peaks are obtained by fitting the 1000 ~ 1800 cm-1 peaks, which indicate that coal contains ash, $–CH_2$ and $–CH_3$, hydrogen-bonded carbonyl groups; Aromatic hydrocarbons with -O- substitution C=C. In Fig. 4 (c), there are two obvious peaks after peak fitting treatment, which represent cycloalkane or aliphatic hydrocarbon CH_3. In Fig. 4 (d), there is a strong absorption peak at about 3430.24 cm^{-1},

Table 3 Parameters of absorption peaks in infrared spectrum of HY coal sample.

Figure	Number	Peak position / cm^{-1}	Peak width / cm^{-1}	Peak type	Area	Relative area /%	Attribution
a	1	750.13	23.72	Gaussian	91.08	37.03	1, 2-substituted aromatic hydrocarbons
	2	799.84	32.86	Gaussian	109.11	44.36	1, 2, 4-substituted aromatic hydrocarbon CH
	3	869.20	20.84	Gaussian	45.78	18.61	1, 2, 4-substituted aromatic hydrocarbon CH
b	1	1028.37	51.16	Gaussian	537.41	26.48	Ash content
	2	1098.95	43.36	Gaussian	249.31	12.28	C—O of phenols, alcohols, ethers and esters
	3	1186.60	62.95	Gaussian	138.78	6.84	C—O of phenols, alcohols, ethers and esters
	4	1385.88	72.47	Gaussian	73.52	3.62	–CH_3 symmetric deformation vibration
	5	1440.69	36.18	Gaussian	136.06	6.70	–CH_2 and-CH_3, inorganic carbonates
	6	1611.39	75.16	Gaussian	894.46	44.07	Carbonyl; -O-substituted aromatic hydrocarbons C═C
c	1	2854.59	45.34	Gaussian	120.61	27.49	Cycloalkane or aliphatic hydrocarbon CH_3
	2	2920.69	66.19	Gaussian	318.16	72.51	Cycloalkane or aliphatic hydrocarbon CH_3
d	1	3430.24	254.85	Gaussian	5414.69	100	Hydroxyl

which is mainly due to the chemical structure of coal containing –OH. To sum up, the infrared peak fitting effect of this coal sample is ideal, and the type of functional groups and the number of functional groups in its coal molecular structure can be basically determined.

By fitting the infrared spectrum of 1800 ~ 1000 cm^{-1}, it can be concluded that the main forms of oxygen in the molecular structure of raw coal of Hongyang No. 2 Mine are ether, phenol and carbonyl. By fitting the infrared spectrum of 3000–2800 cm^{-1}, it can be concluded that the fatty chain in the molecular structure of the raw coal of Hongyang No. 2 Mine is mainly methylene and methylene.

3.2. ^{13}C NMR analysis

^{13}C NMR spectra can be divided into four peaks according to the chemical functional groups of coal, and different chemical shift intervals correspond to different peaks, which are the first peak 0 ~ 60 ppm and lipid carbon peak respectively; The second peak is 60 ~ 90 ppm, and the ether oxygen peak; The third peak is 90 ~ 165 ppm, aromatic carbon peak; The fourth peak is about 200 ppm, and the carbonyl peak (Ge et al., 2017; Fan et al., 2017).

Choose the appropriate peak points, and the ^{13}C NMR spectra for peak fitting processing (using Peakfit software). According to chemical attribution, 12 structural parameters of coal samples are calculated, including (Castro-Marcano et al., 2012; Painter et al., 1987; Li et al., 2013):

f_a- protonated aromatic carbon + bridged aromatic carbon + side-supported aromatic carbon + oxygen substituted aromatic carbon + carbonyl carbon；.

f_{al}- all sp^3 hybrid carbon；.

f_a^c- carboxyl or carbonyl carbon, δ greater than 165；.

$f_a^{\prime}$- aromatic carbon, δ is 100 ~ 165；.

f_a^H- protonated aromatic carbon, δ is 100 ~ 129；.

f_a^N– Aprotonated aromatic carbon, δ is 129 ~ 165；.

f_a^P- oxygen hydroxyl group or other oxygen substituted carbon to form aromatic ring, δ is 148 ~ 165（150 ~ 165）；.

f_a^S- side aromatic carbon, δ is 137 ~ 148 or 135 ~ 150；.

f_a^B- bridged aromatic carbon, δ is 129 ~ 137；.

f_{al}^*- arylmethyl + aliphatic methyl；.

f_{al}^H- methylene, methylene, quaternary carbon；.

f_{al}^O- oxygen grafted carbon, δ为50 ~ 90；.

$f_{al} = 100 - f_a$

Combined with formula (1), the average X_{BP} of aromatic ring polycondensation degree is calculated.

$$X_{BP} = f_a^B/(f_a^H + f_a^P + f_a^S) \quad (1)$$

The ^{13}C NMR spectra of coal samples obtained from experiments and their peak fitting results are shown in Fig. 5. There are five obvious peaks in the ^{13}C NMR spectra of coal samples, the first peak is about 20 ppm, the second peak is about 33 ppm, the third peak is between 60 ~ 90 ppm, the fourth peak is between 160 ~ 190 ppm, and the fifth peak is between 210 ~ 220 ppm. Combined with Table 4, it can be seen from the analysis that the coal samples contain intracyclic oxygrease carbon, methylene, protonated aromatic carbon, carboxyl carbon and carbonyl carbon, etc.

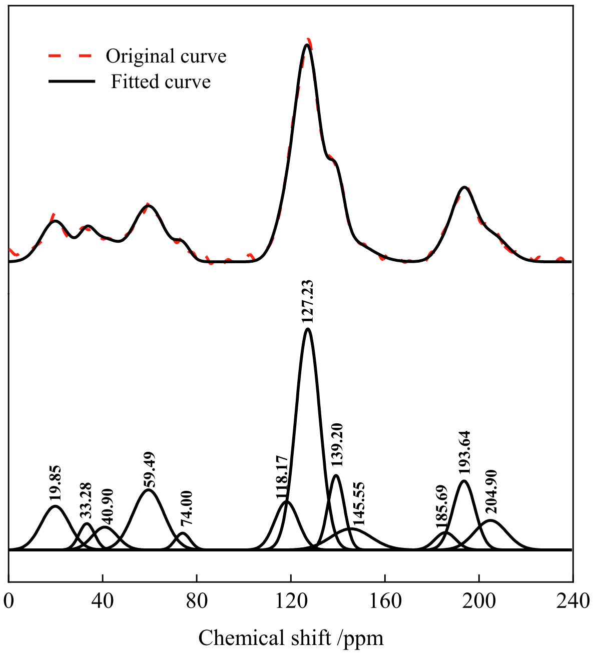

Fig. 5 ^{13}C NMR of coal samples and peak fitting.

Table 4 Peak fitting data of ^{13}C NMR of coal samples.

Number	Chemical shift / ppm	Peak type	Peak width	Area	Relative area / %	Attribution
1	19.85	Gaussian	14.05	9.514e + 08	7.81	Aromatic methyl
2	33.28	Gaussian	7.81	3.201e + 08	2.63	Methylene
3	40.90	Gaussian	12.66	4.478e + 08	3.68	Quaternary carbon, methylene carbon
4	59.49	Gaussian	15.51	1.443e + 09	11.85	Oxygen-grafted methyl and oxygen-grafted methylene carbon
5	74.00	Gaussian	7.54	1.96e + 08	1.61	Intracyclic oxygen grafted carbon
6	119.91	Gaussian	12.51	1.39e + 09	11.41	Protonated aromatic carbon
7	127.76	Gaussian	11.32	3.619e + 09	29.71	Aprotonated aromatic carbon
8	138.81	Gaussian	8.08	9.857e + 08	8.09	Bridged aromatic carbon
9	144.27	Gaussian	12.79	4.458e + 08	3.66	Side-supported aromatic carbon
10	154.93	Gaussian	16.15	1.833e + 08	1.50	Oxygen substituted aromatic carbon
11	188.02	Gaussian	9.46	4.057e + 08	3.33	Carboxyl carbon
12	194.35	Gaussian	7.35	4.732e + 08	3.88	Carbonyl carbon
13	200.01	Gaussian	21.53	1.321e + 09	10.84	Carbonyl carbon

From the intensity of the peak, aromatic carbon is the main one, and the content of other types of carbon is relatively small.

By analyzing the functional group attribution of the above coal samples and synthesizing the data such as half peak width and peak area obtained by peak fitting, the structural parameters of coal samples can be obtained, and the detailed parameters are shown in Table 5.

According to formula (1), the X_{BP} value of coal sample is 0.17. The number of benzene rings and polycondensation degree of coal sample can be judged by this value, and the size of aromatic rings can be calculated.

3.3. Construction of coal molecules

According to the atomic ratio of coal sample, assuming that the number of carbon atoms in coal molecular structure is ×, the molecular formula of coal sample can be given as $C_xH_{0.6117x}O_{0.2194x}N_{0.0141x}S_{0.0094x}$. Scholars have studied the structure and molecular weight of coal molecules, which shows that the molecular weight of coal is 2000 ~ 3000, and the number of atoms is an integer. The molecular weight of coal sample is calculated by formula (2) as follows:

$$M = 12x + 0.6117x + 16 \times 0.2194x + 14 \times 0.0141x + 32 \times 0.0094x \qquad (2)$$

The molecular formula of coal sample is $C_{128}H_{78}O_{18}N_2S$, M = 2122.

3.3.1. Determination of aromatic structure type

Aromatic structure accounts for most of the whole coal molecular structure. The better the coal quality, the greater the proportion of aromatic structure and naphthene in coal, and the higher the degree of polycondensation. The carbon-hydrogen ratio and the calculated X_{BP} in elemental analysis are important indexes reflecting the degree of polycondensation of aromatic structure in coal molecules, and the X_{BP} of HY coal molecule is 0.17. For aromatic structures, X_{BP} of benzene is 0, X_{BP} of naphthalene is 0.25, or X_{BP} of phenanthrene is 0.4,

Table 5 Structural parameters of HY coal sample.

f_a	f_{al}	f_a^c	f_a'	f_a^H	f_a^N	f_a^P	f_a^S	f_a^B	f_{al}^*	f_{al}^H	f_{al}^O
69.09	27.58	14.72	54.37	41.12	13.25	1.50	3.66	8.09	7.81	6.31	13.46

Table 6 Types of aromatic structural units of coal samples.

Structure type	X_{BP}	Number	Structure type	X_{BP}	Number
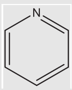	0	1	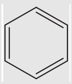	0	1
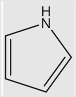	0	1	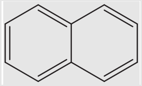	0.25	6
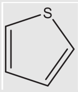	0	1			

X_{BP} of tetraphenyl is 0.5, and X_{BP} of pentaphenol is 0.57 (Qiao et al., 2019; Kawashima and Takahashi, 2001). When establishing the molecular structure of coal, the appropriate aromatic structure should be selected. The appropriate type and quantity should be matched to make the average X_{BP} as close as possible to the X_{BP} of coal molecule. According to the XBP of coal to determine the types and numbers of various aromatic structures in the coal molecules, but also comprehensive consideration of nitrogen and sulfur aromatic structures, pyrrole, pyridine and thiophene.

Through the consideration of X_{BP}, the amount of various aromatic structures in the construction of coal molecules in coal was determined. As shown in Table 6, pyrrole, pyridine, and thiophene structures with aromatic properties are listed separately, and most of them bridge to other aromatic structures in coal molecules.

3.3.2. Determination of fat structure type

The aliphatic carbon in coal is mainly in the form of branch chain or linked aromatic ring, which exists in the form of aliphatic ring, side chain or bridging carbon. The lower the metamorphic degree of coal, the longer the length of alkane side chain in molecular structure (Qiao et al., 2018; Trewhella et al., 1986; Qin et al., 1998). The aromatic ratio of coal sample is 54.37 %. The total number of aromatic carbon is 70, the total number of carbon atoms is 129, and the number of aliphatic carbon atoms is 68. The proportion of f_{al}^{H}, f_{al}^{O}, and f_{al}^{*} is 6.31 %, 13.46 % and 7.81 % respectively. It can be seen that

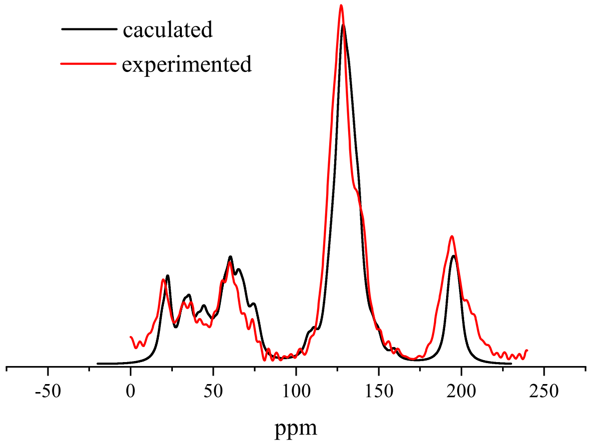

Fig. 6 Comparison of ^{13}C NMR of HY coal model.

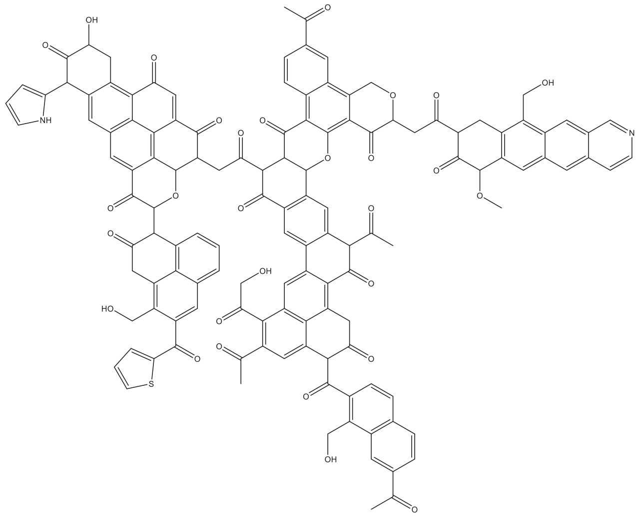

Fig. 7 Macromolecular two-dimensional structure model of HY coal.

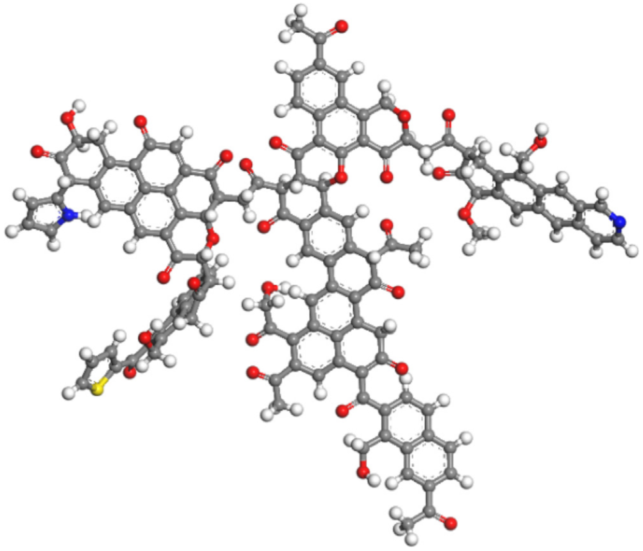

Fig. 8 Macromolecular three-dimensional structure model of HY coal.

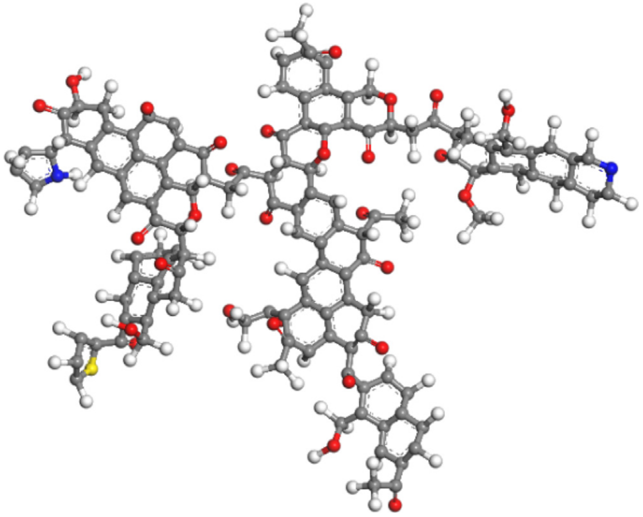

Fig. 9 Optimized molecular structure of coal.

Table 7 Parameter Setting of Molecular Structure Optimization.

Precision	Fine
Force field	COMPASSⅡ
Electric field	Use current
Electrostatic convergence	Atom based
Van der Waals convergence	Atom based

Table 8 Parameters of coal molecular model.

Coal sample	Molecular formula	Molecular weight	Element content /%				
			C	H	O	N	S
HY	$C_{129}H_{88}O_{29}N_2S$	2160	71.66	4.07	21.12	1.20	1.48

Table 9 Comparison elemental analysis between molecular model and test of coal samples.

Element	C	H	O	N	S
Experimented	72.19	3.68	21.12	1.20	1.81
Calculated	71.66	4.07	21.12	1.20	1.48
Deviation	0.007	0.106	0.017	0.083	0.182

methyl, methylene, methylene and quaternary carbon are more in the molecular configuration of coal.

3.3.3. *Determination of the remaining heteroatom types*

The content of N in coal is 1 % ~ 2 %, and the content of N in the form of pyridine ring or pyrrole ring accounts for about 50 % ~ 75 % of the total N content (Niekerk and Mathews, 2010). Thiophene, sulfoxide sulfur, sulfone sulfur, and mercaptan thiophenol are the main forms of organic sulfur in coal samples (Gao et al., 2018). According to the atomic ratio in elemental analysis and the total number of C atoms calculated by ^{13}C NMR, the number of N and S atoms can be calculated. The calculation shows that the number of N atoms is 2 and the number of S atoms is 1. There is one pyridine, one pyrrole, and one thiophene in the molecular configuration.

3.3.4. *Molecular structure model of coal*

Based on the results of aromaticity, structural unit, and elemental analysis, the macromolecular structure model of coal can be constructed. The molecular structure of coal is preliminarily plotted by MS software, and the results are shown in Fig. 6. The ^{13}C NMR spectrum of the macromolecular structure model was calculated by MestReNova software, and compared with the experimental spectrum shown in Fig. 6, it was consistent with the experimental ^{13}C NMR spectrum. The macromolecular two-dimensional structure model of HY coal is obtained, which is shown in Fig. 7. Three-dimensional macromolecular structure model of HY coal is shown in Fig. 8.

Forcite module of MS software was used to optimize the structure and energy of the modified molecular model, so that the molecular structure can reach a stable conformation. The final molecular structure model of coal samples is shown in Fig. 9. The parameter settings in the process of molecular structure optimization are shown in Table 7. The molecular weight and element contents of coal samples are shown in Table 8.

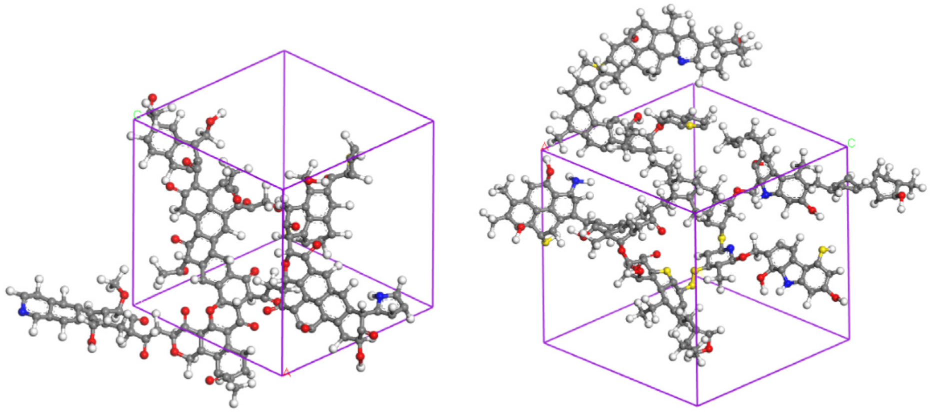

(a) HY (b)Wiser Bituminous coal

Fig. 10 Molecular structure model of coal.

Table 10 Structural parameters of the Wiser bituminous coal macromolecular model.

Molecular formula	Molecular weight	Element content				
		C	H	O	N	S
$C_{192}H_{165}O_{20}N_5S_8$	3115	73.96	10.27	5.30	2.25	8.22

Table 9 shows the error analysis between the coal molecular model and elemental analysis in HY Mine. It can be seen that each element corresponds well.

3.4. Analysis of oxygen absorption characteristics of coal molecular structure in Hongyang No.2 mine

3.4.1. GCMC simulation

The Amorphous Cell module was used to construct the periodic structure, as shown in Fig. 10(a). In this manuscript, the Wiser bituminous coal model was selected as a comparison, as shown in Fig. 10 (b). The structural parameters of the Wiser model are shown in Table 10.

The coal molecular model was optimized geometrically and energetically. Finally, the coal molecular structure with the lowest energy was obtained. The COMPASSII force field was used to optimize the structure geometry, anneal, and then carried out molecular dynamics.

The density change diagram of HY coal model is shown in Fig. 11. The average density of bituminous coal is 1.27 g/cm^3 after 50 ps calculation (the actual density of bituminous coal is between 1.2 and 1.4 g/cm^3), which shows that the molecular structure of the constructed coal is reasonable.

3.4.2. Adsorption isotherm and heat of adsorption

Based on the coal molecular structure model constructed in Fig. 10, Sorption module was used to calculate adsorption isotherms (temperature 293 ~ 333 K, pressure 0 ~ 10 MPa).

The adsorption isotherms of O_2 at different temperatures (293 ~ 333 K) are shown in Fig. 12, and both HY model and Wiser model show the same trend. When the pressure is less than 8Mpa, the average adsorption capacity gradually increases with the increase of pressure. However, when the pressure approaches 10Mpa, the increase rate becomes flat. It is found that as the temperature increases, the corresponding adsorption of O_2 decreases, which indicates that the adsorption of O_2 is an exothermic process. When the pressure is the same, the adsorption capacity of Wiser model is less than that of HY coal model. Compared with Wiser model, HY coal has higher content of oxygenated aliphatic hydrocarbons and lower condensation degree of polycyclic aromatic hydrocarbons. Therefore, it has stronger physical adsorption capacity of O_2. The analysis of physical adsorption parameters in section 3.4.4 shows that hydroxyl, ether bond and carbonyl group have stronger physical adsorption capacity of O_2.

The heat of physical adsorption is generated by the Vanderbilt energy of the interaction between coal and O_2. The relationship between adsorption heat of O_2 and adsorption capacity is shown in Fig. 13. The adsorption heat of O_2 is between 7.5 and 9.5 kJ/mol (less than 42 kJ/mol), indicating that physical adsorption is dominant. The adsorption heat of O_2 increases with the decrease of adsorption amount and the increase of temperature, indicating that the van der Waals force between O_2 and coal molecules decreases with the increase of temperature. The accumulation of isothermal adsorption heat provides the initial energy of the oxidation reaction, and the increase of coal temperature caused by physical adsorption will further accelerate the oxidation reaction. When the amount of O_2 adsorbed is the same, the adsorption

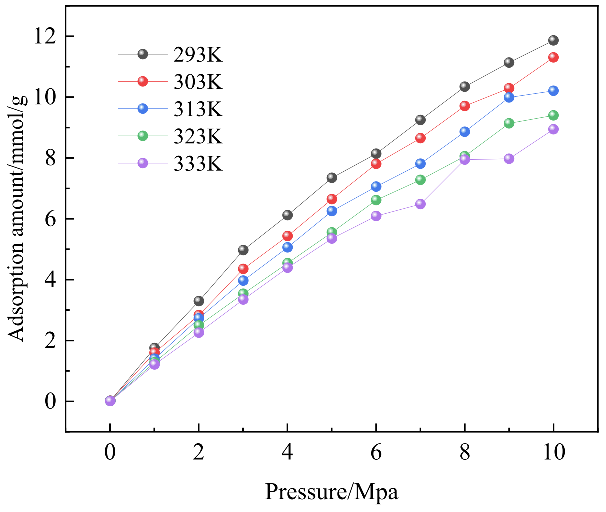

(a) HY

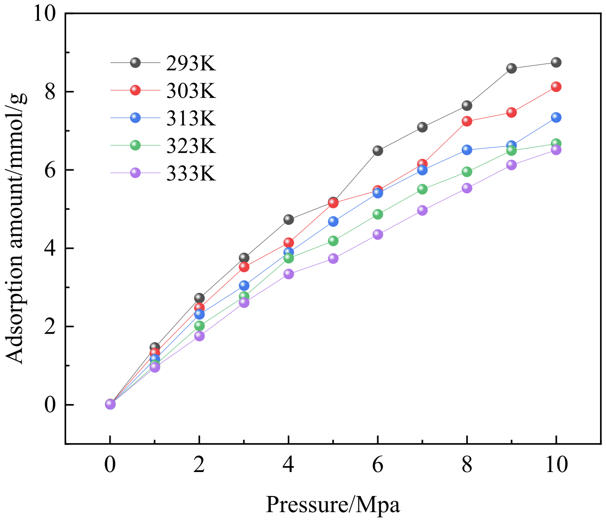

(b) Wiser

Fig. 12 Adsorption isotherms of O_2 at different temperatures.

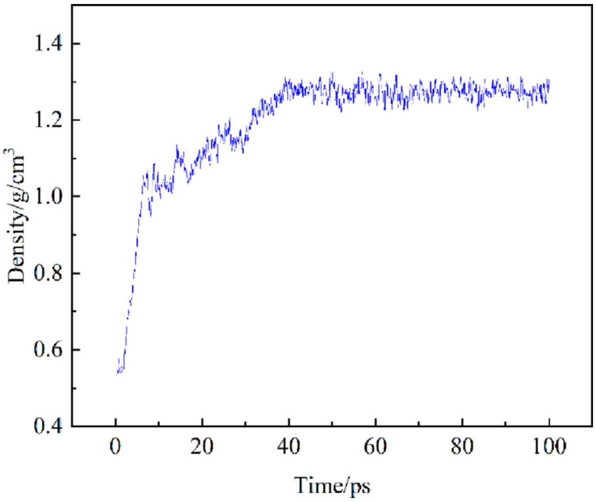

Fig. 11 Density change of HY coal model.

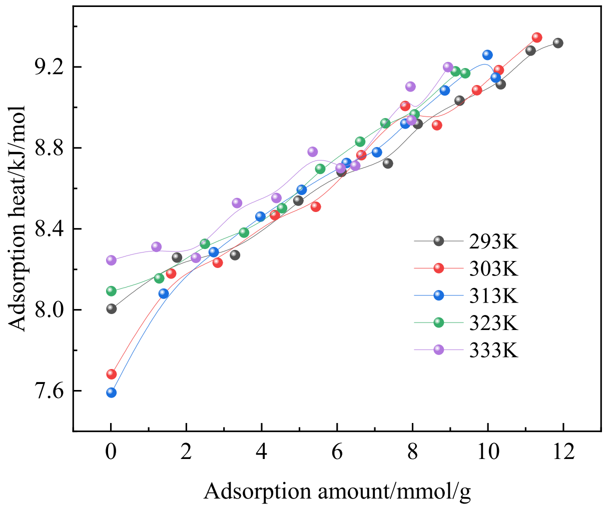

(a) HY

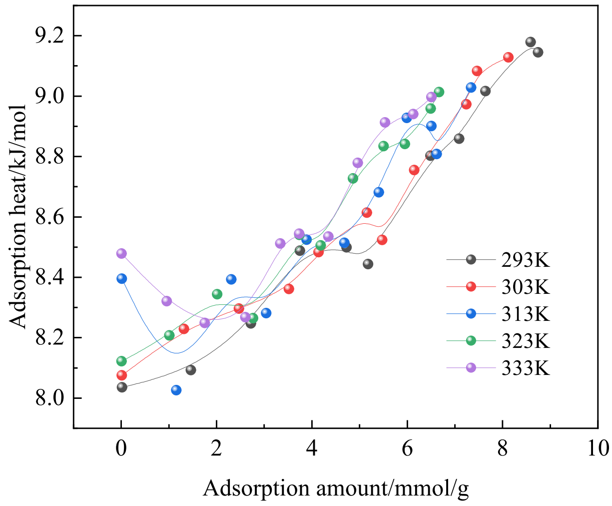

(b) Wiser

Fig. 13 Relationship between adsorption heat of O_2 and adsorption capacity.

heat of Wiser model is less than that of HY coal model, which indicates that the oxygen absorption capacity of HY coal model is greater than that of Wiser model.

3.4.3. Giant potential

To further study the properties of the physical adsorption heat of O_2, the change of interaction energy during physical adsorption was analyzed, as shown in Fig. 14.

Molecular simulation shows that only van der Waal energy is involved in the interaction between coal molecules and O_2 during physical adsorption. This indicates that O_2 is physically adsorbed in coal by the van der Waals force. As more O_2 is adsorbed, the van der Waals energy decreases, which indicates that the physisorption process is exothermic. When the amount of O_2 adsorbed is the same, the van der Waals energy of Wiser model is less than that of HY coal model, which further proves that the oxygen absorption capacity of HY coal model is greater than that of Wiser model.

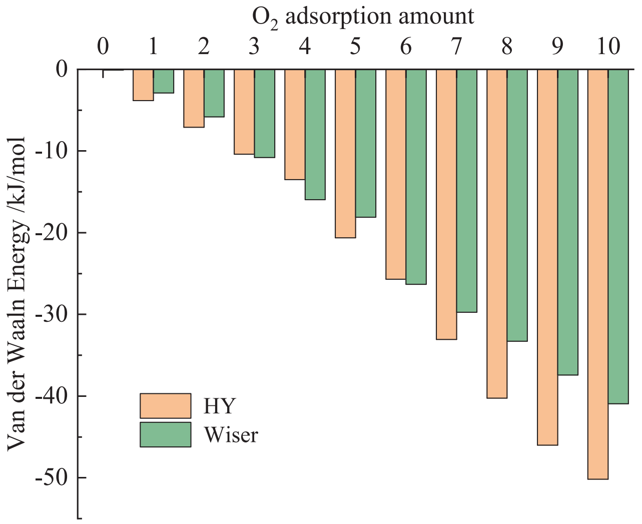

Fig. 14 Relationship between van der Waals energy and O_2 quantity.

3.4.4. Quantum chemical computation

To further study the physical adsorption capacity of O_2 by different functional groups of coal molecules, the physical adsorption parameters of O_2 adsorption by various functional structural units on coal surface were calculated based on quantum chemistry, including adsorption energy, adsorption equilibrium distance and Milliken charge transfer.

The Dmol3 module in MS software was used for quantum chemistry calculation, and the task item was set as Geometry Optimization with fine precision. In the calculation of electronic structure, the PWC functional form of LDA or PWE/PW91 functional form of GGA was used for electron exchange interaction. In order to reduce the disadvantage that GGA functional can not accurately describe non-covalent forces (hydrogen bond and van der Waals force), Grimme method of PWE functional and OBS method of PW91 functional were used for dispersion correction of DFT respectively (Jia et al., 2011). All Electron and DNP base groups were used to describe the nuclear and valence electrons, respectively. The Basis file was 3.5, the orbit cutoff accuracy was set to fine, the integration accuracy and SCF tolerance were set to 1 × 10–6, and the maximum SCF period was 1000.

In order to simplify the calculation, small molecular fragments at each adsorption site were constructed, and their adsorption parameters were analyzed.

The stable adsorption configuration of O_2 at different adsorption sites is shown in Fig. 15, and the physical adsorption parameters of O_2 molecules are listed in Table 11. It can be seen that hydroxyl group (2.992 kcal/mol) and ether bond (2.979 kcal/mol) have lower physical adsorption energy values, and they have higher physical adsorption capacity on O_2. The physical adsorption equilibrium distance between hydroxyl (2.338) and methyl (2.914) and O_2 is relatively small, while the physical adsorption distance between other adsorption sites and O_2 is greater than 3 Å. Milliken charge transfer represents the polarization degree of O_2 in physical adsorption. Hydroxyl group (0.043 e) has higher charge, followed by carbonyl group (0.025 e), methyl group (0.027 e) and ether bond (0.018 e), which indicates that O_2 is adsorbed more stably near

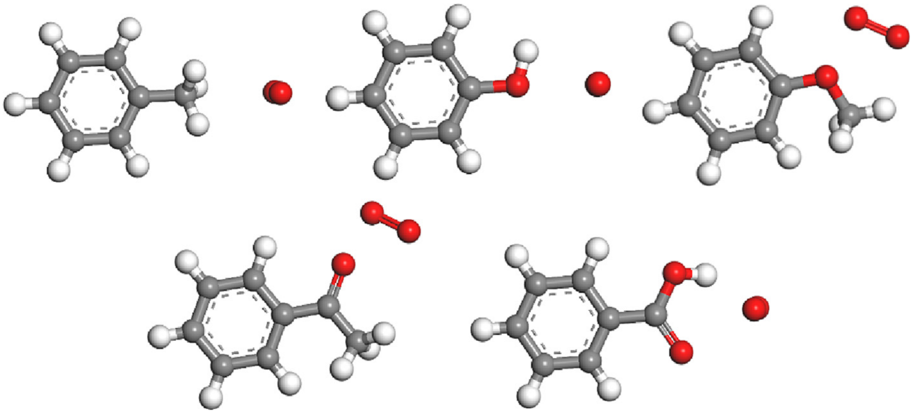

Fig. 15 Stable adsorption configuration of molecular O_2 at different adsorption sites.

Table 11 Adsorption parameters of molecular O_2 at different adsorption sites.

Adsorption site	Direction	Adsorption energy /kcal/mol	Balance distance /Å	Charge transfer /e
$-CH_3$	Parallel	−1.722	2.914	−0.022
–OH	Parallel	−2.992	2.338	−0.043
-C—O—C	Parallel	−2.979	3.218	−0.018
-C═O	Parallel	−2.475	3.095	−0.027
–COOH	Parallel	−2.187	3.046	−0.013

these adsorption sites. The smaller the physisorption energy and charge transfer value of O_2 in parallel adsorption configuration, the easier it is for O_2 to physisorption around adsorption sites in parallel adsorption configuration. Therefore, hydroxyl group, ether bond and carbonyl group are active groups for physisorption of O_2.

The adsorption affinity of different functional groups of O_2 is obviously different, which provides energy for the gradual self-activation reaction of coal spontaneous combustion. The simulation results show that the heat released by physical adsorption can trigger the spontaneous combustion of coal. Therefore, it is possible to design inhibitors closer to the reactive groups in coal to reduce the physical adsorption heat and fundamentally prevent coal from spontaneous combustion.

4. Conclusion

(1) According to the ^{13}C NMR parameters, the ratio of aromatic bridge carbon to weekly carbon in coal molecular structure is calculated to be 0.17. The aromatic compounds in HY coal samples are mainly naphthalene ring structures. Oxygen atoms exist in the form of carbonyl, hydroxyl, and ether bonds, nitrogen atoms exist in the form of pyridine and pyrrole respectively, and sulfur atoms exist in the form of thiophene.

(2) Using ChemDraw, Chem3D and MestReNova, the structure model which fits well with the 13C NMR spectra of HY coal was constructed; The molecular formula of HY coal is $C_{129}H_{88}O_{29}N_2S$ and the molecular weight is 2160.

(3) The adsorption capacity of the Wiser model is less than that of HY coal model. Compared with Wiser model, HY coal has higher content of oxygenated aliphatic hydrocarbons and lower condensation degree of polycyclic aromatic hydrocarbons. Due to the stronger physical adsorption capacity of hydroxyl, ether bond, and carbonyl on O_2, HY Mine has stronger physical adsorption capacity on O_2.

(4) The adsorption ability of different functional groups to O_2 is obviously different, which provides energy for the gradual self-activation reaction of coal spontaneous combustion. It is possible to design inhibitors closer to the reactive groups in coal to reduce the physical adsorption heat and fundamentally prevent coal from spontaneous combustion.

CRediT authorship contribution statement

Cong Ding: Supervision, Funding acquisition. **Zongxiang Li:** Data curation. **Dongjie Hu:** Data curation, Supervision. **Chuntong Miao:** . **Bing Lu:** Supervision. **Dameng Gao:** .

Declaration of Competing Interest

The authors declare that they have no known competing financial interests or personal relationships that could have appeared to influence the work reported in this paper.

Acknowledgments

The authors acknowledge the financial support from the National Natural Science Foundation of China (51774170).

References

Bhoi, S., Banerjee, T., Mohanty, K., 2014. Molecular dynamic simulation of spontaneous combustion and pyrolysis of brown coal using Reax FF. Fuel 136, 326–333.

Castro-Marcano, Vladislav V. Lobodin, Ryan P. Rodgers, et al. A molecular model for Illinois No. 6 Argonne Premium coal: Moving toward capturing the continuum structure. Fuel 2012; 95:35-49

Cheng, G., Li, Y.L., Zhang, M.N., Cao, Y.J., 2021. Simulation of the adsorption behavior of $CO_2/N_2/O_2$ and H_2O molecules in lignite. J. China Coal Soc. 46 (S2), 960–969.

Fan, Y., Hou, Y.C., Wu, W.Z., et al, 2017. A new insight into the structure of Huolinhe lignite based on the yields of benzene carboxylic acids. Fuel 189, 408–418.

Gao, M.J., Li, X.X., Guo, L., 2018. Pyrolysis simulations of Fugu coal by large-scale ReaxFF molecular dynamics. Fuel Process. Technol. 178, 197–205.

Ge, T., Zhang, M.X., Ma, X.M., 2017. XPS and FTIR spectroscopy characterization about the structure of coking coal in Xinyang. Spectrosc. Spectr. Anal. 37 (8), 2406–2411.

Given, P.H., 1959. Structure of bituminous coals: evidence from distribution of hydrogen. Nature 184, 980–981.

He, X., Wang, W.F., Zhang, X.X., et al, 2021. Distribution characteristics and differences of oxygen-containing functional groups in macerals of low-rank coal. J. China Coal Soc. 46 (9), 2804–2812.

Hong, D.K., Liu, L., Wang, C.B., et al, 2021. Construction of a coal char model and its combustion and gasification characteristics: molecular dynamic simulations based on ReaxFF. Fuel 300.

Jia, J.B., Zeng, F.G., Sun, B.L., 2011. Construction and modification of ^{13}C-NMR spectra of macromolecular structure model of Shandong 2–2 coal mirror group. J. Fuel Chem. Technol. 39 (9), 652–657.

Jiang, W.P., Cui, Y.J., Zhang, Q., et al, 2006. The quantum chemical study on the coal surface interacting with CH_4 and CO_2. J. China Coal Soc. 31 (2), 237–240.

Jiang, Y., Zong, P.J., Tian, B., et al, 2019. Pyrolysis behaviors and product distribution of Shenmu coal at high heating rate: A study using TG-FTIR and Py-GC/MS. Energ. Conver. Manage. 179, 72–80.

Kawashima, H., Takahashi, T., 2001. Modification of model structures of Upper Freeport coal extracts using ^{13}C-NMR chemical shift calculations. Energy Fuel 15 (3), 591–598.

Li, W., Zhu, Y.M., Chen, S.B., et al, 2013. Research on the structural characteristics of vitrinite in different coal ranks. Fuel 107 (9), 647–652.

Lou, H.Z., Jia, T.G., 2020. Competitive adsorption differences during coal spontaneous combustion process in noble gas atmosphere. China Saf. Sci. J. 30 (4), 60–67.

Mathews, J.P., Duin, A.C.T.V., Chaffee, A.L., 2011. The utility of coal molecular models. Fuel Process. Technol. 92 (4), 718–728.

Meng, J.Q., Zhong, R.Q., Li, S.C., et al, 2018. Molecular model construction and study of gas adsorption of Zhaozhuang coal. Energy Fuel 32 (9), 9727–9737.

Niekerk, D.V., Mathews, J.P., 2010. Molecular representations of Permian-aged vitrinite-rich and inertinite-rich south African coals. Fue 89 (1), 73–82.

Painter, P.C., Sobkwiak, M., Youtcheff, J., 1987. FTIR study of hydrogen bonding in coal. Fuel 66 (7), 973–978.

Qiao, L., Deng, C.B., Zhang, X., et al, 2018. Effect of soaking on the oxidation activation energy and thermal effect of coal. J. China Coal Soc. 43 (9), 2518–2524.

Qiao, L., Deng, C., Dai, F., et al, 2019. Experimental study on a metal-chelating agent inhibiting spontaneous combustion of coal. Energy Fuel 33 (9), 9232–9240.

Qiao, L., Deng, C., Lu, B., et al, 2022. Study on calcium catalyzes coal spontaneous combustion. Fuel 307, 121884.

Qin, Y., Jiang, B., Song, D.Y., et al, 1998. Characteristics and mechanism on the ^{13}C-NMR evolution of the carbon structure in the high-rank coals. J. China Coal Soc. 23 (6), 634–638.

Shinn JH. Visualization of complex hydrocarbon reaction systems. Preprints of Papers American Chemical Society Division of Fuel Chemistry 1996; 41(6): 418

Trewhella, M.J., Popletti, J.F., Grint, A., 1986. Structure of green river oil shale kerogen: determination using solid state ^{13}C-NMR spectroscopy. Fuel 65 (4), 541–546.

Wiser, W.H., 1984. Conversion of bituminous coal to liquids and gases: chemistry and representative processes. Springer, Magnetic Resonance. Netherlands.

Wu, S.Y., Jin, Z.X., Deng, C.B., 2019. Molecular simulation of coal-fired plant flue gas competitive adsorption and diffusion on coal. Fuel 239, 87–96.

Xia, Y.C., Yang, Z.L., Zhang, R., et al, 2019. Enhancement of the surface hydrophobicity of low-rank coal by adsorbing DTAB: An experimental and molecular dynamics simulation study. Fuel 239, 145–152.

Xu, L., 2012. World coal resource supply and demand analysis. Coal Geol. China 24 (6), 74–76.

Zeng, Q., Pu, Y., Cao, Z.M., 2018. Kinetics of oxidation and spontaneous combustion of major super-thick coal seam in Eastern Junggar Coalfield, Xinjiang, China. J. Loss Prev. Process Ind. 56, 128–136.

Zhang, Z., Kang, Q., Wei, S., et al, 2017. Large-scale molecular model construction of xishan bituminous coal. Energy Fuel 31, 1310–1317.

Zhang, J., Wang, J.R., Zhang, C.H., et al, 2021. Molecular simulation of C_2H_4 /CO_2 /N_2 /O_2 adsorption characteristics in lignite and anthracite. AIP Adv. 11, 085205.

Zhang, X.D., Zhang, P., 2014. Characteristics of XRD parameter for different ranks of coals under fractional extraction and its evolution mechanism. J. China Coal Soc. 39 (5), 941–946.